AJNR

Identification of the Distal Dural Ring with Use of Fusion Images with 3D-MR Cisternography and MR Angiography: Application to Paraclinoid Aneurysms

Y. Watanabe, T. Nakazawa, N. Yamada, M. Higashi, T. Hishikawa, S. Miyamoto and H. Naito

Y. Watanabe
T. Nakazawa
N. Yamada
M. Higashi
T. Hishikawa
S. Miyamoto
H. Naito

Identification of the Distal Dural Ring with Use of Fusion Images with 3D-MR Cisternography and MR Angiography: Application to Paraclinoid Aneurysms

BACKGROUND AND PURPOSE: The distal dural ring (DDR) represents the anatomic border between the extradural and intradural internal carotid arteries (ICAs). The purpose of this study was to examine whether 3D-MR cisternography and MR angiography (MRA) fusion images can identify the boundary between the CSF and the cavernous sinus, which might represent the DDR.

MATERIALS AND METHODS: Thirty-six consecutive patients with 39 ICA aneurysms were examined with use of MR fusion images with 3D-cisternography and MRA on a 1.5T unit. Two neuroradiologists evaluated the configuration of the carotid cave and the location of the aneurysms on fusion images and classified them as intradural, transdural, and extradural aneurysms.

RESULTS: The borderline between the CSF and the cavernous sinus was visualized on fusion images in all patients. The carotid cave configuration in 72 ICAs was classified as having no dent ($n = 31$), a shallow dent ($n = 27$), and a deep dent ($n = 14$). The MR fusion images led to the classification of 39 ICA aneurysms as 21 intradural, 6 transdural, and 12 extradural. The interobserver agreement of MR fusion images was excellent ($\kappa = 0.80$).

CONCLUSIONS: Fusion images with 3D-cisternography and MRA yielded clear visualization of the boundary between the suprasellar cistern and cavernous sinus indicating the DDR. This imaging technique may provide additional information in consideration of a treatment option for paraclinoid aneurysms.

The distal dural ring (DDR) is the anatomic border between the intracavernous and supracavernous internal carotid arteries (ICAs), and the DDR is an important landmark to differentiate an intradural paraclinoid aneurysm from an extradural cavernous sinus aneurysm. Paraclinoid aneurysms carry a risk for subarachnoid hemorrhage (SAH), and treatment can be rendered. On the other hand, cavernous sinus aneurysms have limited or no risk for SAH and are usually followed up in asymptomatic patients.

The carotid cave is a small intradural recess at the posteromedial aspect of the DDR, and it has been observed in two thirds of cadavers in 2 studies.[1,2] This recess causes difficulty in differentiating intradural from extradural aneurysms at the medial side of the ICA.[3]

3D-MR cisternography with use of constructive interference in steady state (3D-CISS) can provide high-resolution images with good contrast between the CSF and solid structures.[4,5] However, solid structures such as blood vessels, cranial nerves, and bones are difficult to identify only by 3D-CISS imaging, which imposes a limit on evaluating aneurysms by 3D-CISS imaging. 3D time-of flight (3D-TOF) MRA can demonstrate the artery as a high signal intensity, and this technique is widely applied to evaluate intracranial aneurysms.[6] Recent advances in 3D workstations have facilitated fusing the 2 images of different datasets. Fused CT and MR images have been

used for surgical planning,[7] and fused MRA and 3D cisternography images have been applied to analyze the intracranial blood vessels.[8] Fusion of 3D-CISS and MRA images will theoretically reveal the CSF space and artery, and the boundary where the ICA penetrates the dura mater should be visualized.

This study was undertaken to evaluate whether 3D-CISS and MRA fusion images can identify the borderline between the CSF and the cavernous sinus. We evaluated the configuration of the carotid cave and applied it to differentiate the paraclinoid and cavernous sinus aneurysms.

Materials and Methods

Patients

We prospectively studied MR images of 36 consecutive patients (age range, 26–75 years; mean, 56 years) with unruptured aneurysms at the ICA adjacent to the anterior clinoid process obtained between January 2007 and March 2008. All patients underwent MR imaging with MRA plus 3D-CISS. This study proceeded in accordance with the ethics guidelines of our hospital, and each patient provided informed consent on admission.

MR Imaging and Fusion Method

We obtained all MR images using a standard head coil and a 1.5T system (Magnetom Vision; Siemens, Erlangen, Germany). Both MRA and 3D-CISS sequences were obtained during the same examination. The following parameters were established for the 3D-TOF MRA: TR, 35 ms; TE, 7.6 ms; NEX, 1; flip angle, 20°; slab thickness, 64 mm; partitions, 64; FOV, 20 cm; and matrix, 512×256. The slabs were placed in the axial plane at the center of the sella turca. Cephalad saturation pulses were applied to eliminate venous blood signals. We evaluated the bilateral cavernous sinuses and suprasellar cisterns by
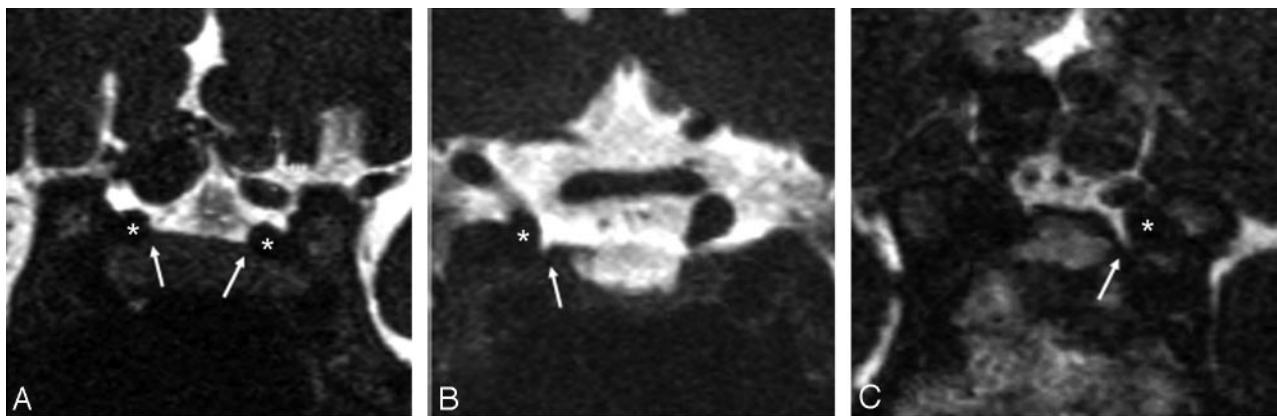
Fig 1. Configuration of the carotid cave (*arrow*) by 3D-CISS coronal images. The depth of the carotid cave is classified as having no dent (*A*), a shallow dent (*B*), and a deep dent (*C*). The asterisk indicates the ICA.
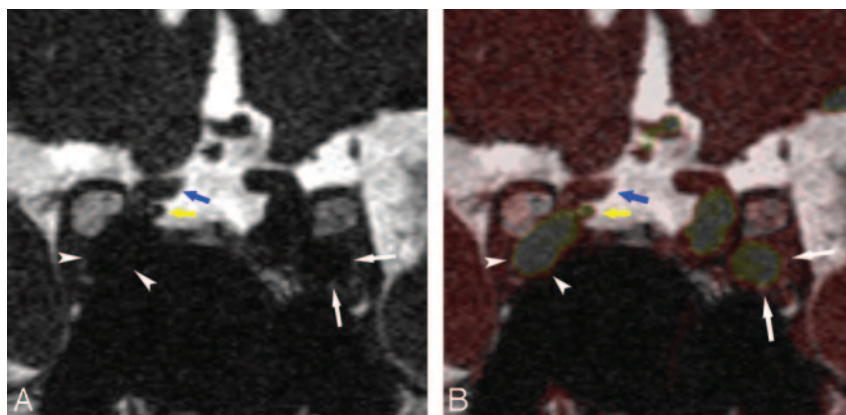

Fig 2. Visualization of the ICA border in the cavernous sinus. On the 3D-CISS image (*A*), the right ICA (*arrowhead*) is rated as grade I (no visible boundary), and the left ICA (*white arrows*) is rated as grade II (vaguely visible boundary). On the fusion image with 3D-CISS and MRA (*B*), both ICAs are rated as grade III (obvious boundary with clear delineation). The optic nerve (*blue arrow*) and ophthalmic artery (*yellow arrow*) were easy to differentiate with fusion image.

coronal imaging with a 3D-CISS sequence (TR, 12 ms; TE, 6.0 ms; NEX, 1; flip angle, 70°) using the following imaging parameters: matrix size, 512 × 314; FOV, 200 mm; and effective section thickness, 0.7 mm.

The MR images were transferred to a 3D workstation (ZioStation; Ziosoft, Tokyo, Japan) and the "multi-data fusion" function was applied, which fuses 2 datasets and allows analysis of multiplanar directions. The software corrected misregistration manually between 2 images by adjusting the positions of one of them in 3D. We displayed the fused images using a choice of several color tables, and we superimposed MRA images in color scale over 3D-CISS images, which were displayed in gray-scale. The mixture ratio of each image component was variable, and it could be easily changed by the reviewers.

Image Analysis

Two neuroradiologists independently analyzed fused multiplanar reconstruction images using a 3D workstation. They compared the position of a given point on 1 plane with its position on 2 other perpendicular planes. Disagreement regarding final conclusions was resolved by consensus. The DDR was defined as a curved plane passing the ICA into the suprasellar CSF space, which was delineated by the boundary between the CSF and roof of the cavernous sinus.

To elucidate the configuration of the carotid cave, the medial edge between the ICA and tuberculum sellae space was classified as the following types: "A," no dent; "B," shallow dent in which the depth

was below the radius of the adjacent ICA; and "C," deep dent in which the depth exceeded the ICA radius (Fig 1).

On the basis of the relationship between the aneurysm and DDR on fusion images, the aneurysms were recorded as intradural, in which the aneurysm was surrounded by CSF and was located distal from the DDR; transdural, in which the portion of the aneurysm was surrounded by CSF and was located on both sides of the DDR; and extradural, in which the aneurysm was located in the cavernous sinus and was proximal to the DDR. To elucidate the visibility of the boundary of the ICAs in the cavernous sinus, 2 neuroradiologists assessed fusion images and 3D-CISS images by using a 3-point scale as follows: grade I, no visible boundary; grade II, vaguely visible boundary; and grade III, obvious boundary with clear delineation (Fig 2).

MRA was independently reviewed on maximum intensity projection and volume rendering (VR) images on the same 3D workstation. The relationship between the neck of the aneurysm and the origin of the ophthalmic artery was evaluated by reviewers. If the aneurysm was located distal to the portion of the ophthalmic artery, the aneurysm was judged as intradural, and if the aneurysm was located proximal to the ophthalmic artery, it was considered extradural.

Statistical Analysis

We evaluated the interobserver agreement for the aneurysmal position, configuration of the carotid cave, and ICA boundary by using the kappa coefficient (κ). Agreement was considered as low, moder-

Differentiation of aneurysms from extradural to intradural by MR fusion images and relationship to the origin of the ophthalmic artery				
	MR Fusion Findings			
Ophthalmic artery	Intradural	Transdural	Extradural	Total
Distal	16	2	1	19
Same level	4	1	3	8
Proximal		3	8	11
Not visible	1			1
Total	21	6	12	39

ate, good, or excellent according to κ values of 0.40 or less, 0.41 to 0.60, 0.61 to 0.80, and 0.80 or more, respectively. We analyzed the score of the ICA visualization in the cavernous sinus on fusion images and 3D-CISS images by using the Wilcoxon signed-rank sum test. All data were analyzed with SPSS software (Chicago, Ill). Statistical significance was established at $P = .05$.

Results

A total of 72 ICAs and 39 aneurysms (maximal diameter: range, 2.3–18 mm; mean, 5.1 mm; median, 4 mm) in 36 patients were evaluated. The border between the suprasellar CSF and the cavernous sinus was visualized for all sides of the ICA on fused images, and this border was considered to represent the DDR.

Regarding the carotid cave configuration (Fig 1), 31 were classified as type A, 27 as type B, and 14 as type C. The interobserver agreement was good ($\kappa = 0.67$). Regarding the visualization of the ICA border in the cavernous sinus (Fig 2), 19 ICAs were classified as grade I, 41 ICAs were classified as grade II, and 12 ICAs were classified as grade III on 3D-CISS images. However, all 72 ICAs were graded as III on fusion images. The ICA border in the cavernous sinus was significantly better visualized on fusion ($P < .01$) than 3D-CISS images, and interobserver agreement on 3D-CISS images was moderate ($\kappa = 0.52$).

The Table summarizes the location of the aneurysms on the basis of fusion images and MRA findings. The MR fusion images led to the classification of 39 ICA aneurysms as 12 extradural (Fig 3), 21 intradural (Fig. 4), and 6 transdural (Fig. 5). The interobserver agreement of MR fusion images was excellent ($\kappa = 0.80$). Eight aneurysms were diagnosed at the same level of the ophthalmic artery, and 1 ophthalmic artery could not be visualized on MRA. One aneurysm, which was located at the distal site of the ophthalmic artery on MRA, was diagnosed as an extradural aneurysm on fusion images (Fig 3).

Eight patients were treated by surgery or by coil embolization: 2 underwent direct surgical clipping, 3 underwent ICA trapping with high-flow external carotid artery-ICA bypass, and 3 underwent coil embolization. The surgical findings of the 5 patients regarding aneurysmal locations were consistent with the MR findings (Fig 6).

Discussion

General Anatomy

The dural ring is surrounded on 3 sides by bony structures: the anterior clinoid process is located laterally, the optic strut anteriorly, and the tuberculum sellae medially. There were no bony structures posteriorly, and the dura matter continued to the diaphragm sellae and posterior clinoid process.[2] The dural ring consists of 2 fibrous rings. The DDR arises from fibers of the superficial dural layer, whereas the proximal ring is located laterally and is related to the deep dural layer, which forms the superior border of the cavernous sinus. The intracavernous segment of the ICA, which is located below the proximal ring, and the ICA appear in the subarachnoid space above the distal ring. The clinoid segment of the ICA is defined as the portion between the proximal ring and the DDR, and it is shaped more like a wedge than a cylinder.[9] The medial side of the DDR forms a pouch known as the carotid cave.[10]

Our study showed that 57% of the ICAs had a pouch on the medial side of the DDR, and 19% of the ICAs had a deep cleft on MR images. A microanatomic study of cadaver specimens by Hitotsumatsu et al[1] found that in 34 (68%) of 50 sides, a carotid cave was located in the posteromedial aspect of the DDR. They classified the cave into 3 types: slit-type (34%) comprising a small thin recess, pocket-type (24%) with a definite dural pouch, and mesh-type (10%) with a meshlike dural roof that is discernable only on microscopic examination. Our MR findings were consistent with these on microsurgical anatomy, and the mesh-type carotid cave was difficult to detect on MR images. Because the presence and depth of the carotid caves varied among patients, differentiation of extradural aneurysms from intradural aneurysms is difficult when bony structures alone are used for reference.[2]

Review of the Literature

The DDR is the anatomic landmark between the extradural and intradural ICA. Discriminating between paraclinoid intradural and extradural cavernous aneurysms is critical when considering treatment options. Some investigators attempted to identify the DDR for differentiation of intradural from extradural ICA aneurysms.[11,12]

The traditional anatomic landmark on digital subtraction angiography for discrimination between paraclinoid and cavernous sinus aneurysms is the origin of the ophthalmic artery[13] or bony structures such as the tuberculum sellae.[2] However, anatomic variations in these markers may cause inaccuracies in locating this junction.

Some studies with 3D-CT angiography were based on the optic strut, which is located in the anterior border of the proximal dural ring.[14,15] Another approach to identify the location of the DDR is to show the borderline of the CSF in the suprasellar cistern, which is considered the location of the dural fold. CT cisternography was once used for preoperative evaluation of paraclinoid aneurysms,[16] but this technique can be time consuming and invasive. Thines et al[11] found that high-resolution T2-weighted MR images can define the inferior limit of the DDR. They used coronal and oblique sagittal planes of T2-weighted images to assess whether paraclinoid aneurysms were located in the intradural or extradural space.[12] Hirai et al[17] identified a boundary between the CSF and the roof of the cavernous sinus by using contrast-enhanced 3D-CISS (CE-3D-CISS) imaging and considered it as the proximal ring. The cavernous sinus was enhanced by contrast medium on CE-3D-CISS images, which allowed differentiation of the ICA in the cavernous sinus, and 9 of 11 paraclinoid aneurysms were accurately diagnosed on the basis of their surgical findings.
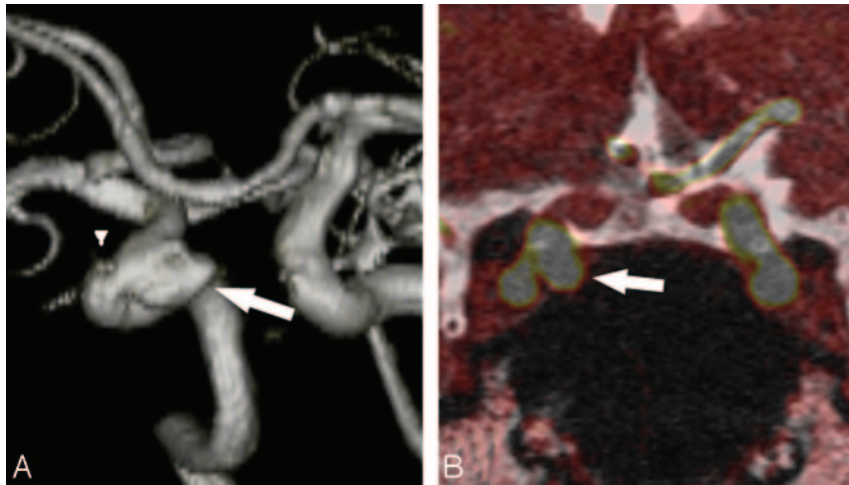
Fig 3. Right ICA aneurysm projection medially. The MRA VR image (*A*) shows that the aneurysm (*arrow*) is located just distal to the ophthalmic artery (*arrowhead*), indicating the aneurysm to be intradural. However, on fusion images (*B*), the aneurysm (*arrow*) dose not contact with the CSF of the suprasellar cistern and was diagnosed as an extradural aneurysm.
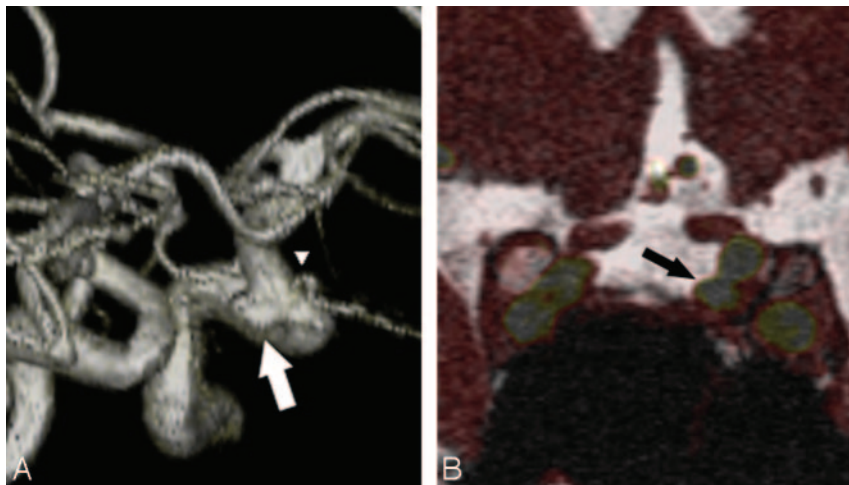

Fig 4. Left ICA aneurysm projection medially. *A,* MRA VR image. *B,* Fusion images. The aneurysm is located at lateral aspect of the ICA, the same level of the origin of the ophthalmic artery. The aneurysm (*arrow*) on the fusion image is faced to the CSF space and is diagnosed as an intradural paraclinoid (carotid cave) aneurysm.
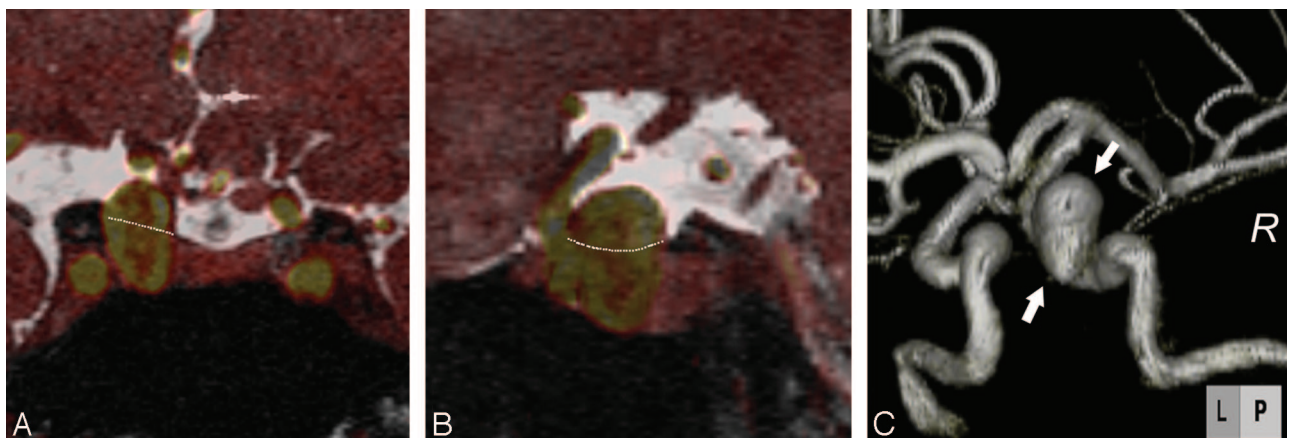

Fig 5. Large right ICA aneurysm. *A,* Fusion coronal image. *B,* Fusion sagittal image. *C,* VR images. The upper dome of the aneurysm contacts to the CSF space, but the lower dome of the aneurysm is seen in the cavernous sinus. The white line is the assumed line of the DDR. This aneurysm (*arrow*) is classified as a transdural type.

Value of MR Fusion and Comparison with the Origin of the Ophthalmic Artery

Our fusion method of 3D-CISS and MRA is analogous in demonstrating the DDR as a border between the CSF and cavernous sinus on 3D-CT cisternography[16] or T2-weighted images.[11] High-resolution images with good contrast to the CSF are rendered by 3D-CISS MR imaging, which could be reconstructed on various planes. However, solid structures such as
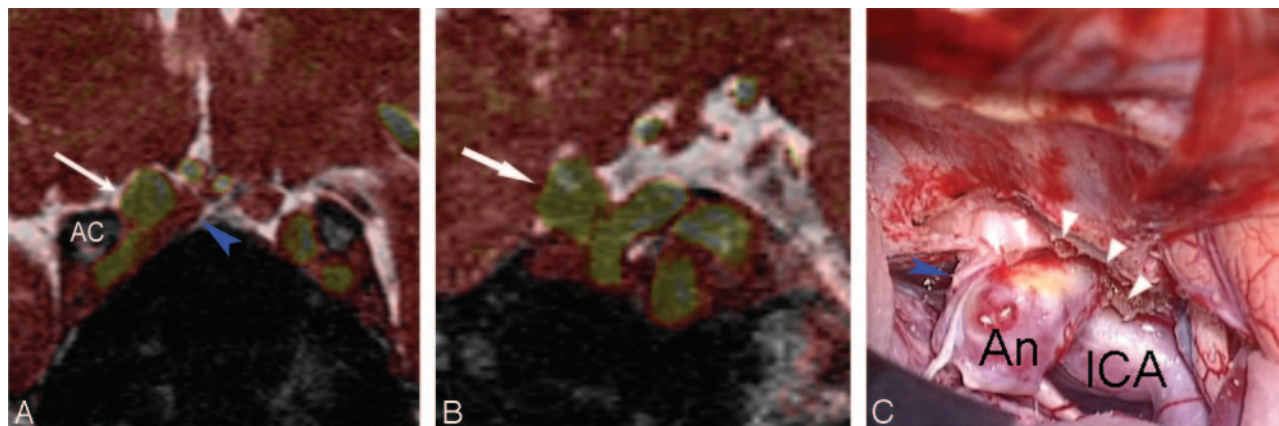
Fig 6. Anterior wall aneurysm of the right ICA. The MR images ([*A*] fusion coronal image and [*B*] fusion sagittal image) show that the aneurysm (*arrow*) is located just distal to the DDR (intradural) and is attached to the anterior clinoid process (AC) laterally. The operative view after removing the anterior clinoid process and sectioning of the DDR shows the aneurysm to be distal to the DDR. An indicates aneurysm; ICA, distal internal carotid artery; *white arrowheads*, tag ends of the DDR; *blue arrowhead*, optic nerve.

blood vessels, cranial nerves, and bones are difficult to differentiate with use of only 3D-CISS images (Fig 2); therefore, we fused MRA to 3D-CISS images to identify the arteries. The recent advance of the 3D workstation makes it possible to analyze and review fusion images. Visualizing the ICA in the cavernous sinus was significantly superior on fusion images than on 3D-CISS images alone, and the artery and aneurysms were easily visualized on fusion images (Fig 2).

Satoh et al[8,18] assessed the vascular anatomy on fusion images by using 3D cisternography and MRA to differentiate infundibular dilation from true aneurysms and to evaluate the perianeurysmal anatomy. This technique is useful to observe the artery and surrounding structures because intraluminal (MRA) and extraluminal (3D cisternography) approaches are combined.

3D-TOF-MRA has the possibility of incomplete visualization of an aneurysm because of slow flow or disturbed flow, especially for large or giant aneurysms. In our series, there were no aneurysms of incomplete visualization with TOF-MRA. Our fusion method basically evaluated the borderline of the aneurysm by 3D-CISS images, which remain nearly unaffected by slow or disturbed flow, and a fused 3D-TOF-source image was used to recognize the artery on the 3D-CISS image. Therefore, the fusion method might be useful to evaluate such incomplete or inaccurate visualized aneurysms with 3D-TOF-MRA.

Punt[13] reported that the origin of ophthalmic artery can be used as the landmark of the intradural ICA. This rule occasionally fails because the origin of ophthalmic artery is extradural in approximately 8% of cases.[9,19] In our study, we evaluated the location of intradural or extradural aneurysms on the basis of the fusion image and origin of ophthalmic artery. The ophthalmic artery generally arises on the anteromedial aspect of the ICA. In our study, 8 aneurysms projected to medial or ventral were diagnosed at the same level of the ophthalmic artery because with these aneurysms it was difficult to determine the positional relationship to the origin of ophthalmic artery. One aneurysm was located distal to the ophthalmic artery origin, but fusion images demonstrated it as an extradural aneurysm (Fig 3).

In our study, 6 aneurysms were denoted as a transdural aneurysm. al-Rodhan et al[20] classified the clinoidal region an-

eurysm into 5 types (including 2 subtypes): Ia, superior hypophyseal aneurysm; Ib, ventral paraclinoid aneurysm; II, ophthalmic aneurysm; III, carotid cave aneurysm; IV, transitional cavernous aneurysm; and V, intracavernous aneurysm. Among these classifications, 3 types have the possibility to be the transdural aneurysm. Transitional cavernous aneurysm (type IV) is defined as their neck arises from the cavernous segment of the ICA, but its dome projects superiorly into the intradural space. A ventral paraclinoid aneurysm (type Ib) projects inferiorly, and the neck arises in the intradural ICA. However, the dome projects extradurally into the cavernous sinus. A carotid cave aneurysm (type III) projects medially, and it sometimes projects into the cavernous sinus. In our series, 4 aneurysms were ventral paraclinoid, 1 was carotid cave, and 1 was a transitional cavernous aneurysm.

Limitations
Our study had some limitations. First, most of the aneurysms in our series were small (< 5 mm), and many of them were followed without treatment. Surgical confirmation was obtained only for 5 patients who were diagnosed as having intradural aneurysms on MR imaging. Recently, many paraclinoid aneurysms, especially carotid cave aneurysms, tended to be treated by coil embolization, and surgical confirmation regarding their exact location is difficult.

Second, we evaluated the border of the CSF and the roof of the cavernous sinus as the landmark of the DDR, but we did not visualize the dura itself. Aneurysms located in the cavernous sinus that projected upward sometimes mimic the transitional type. Conversely, it was difficult to differentiate the intradural or transdural type when ICA ventral aneurysms located intradurally extended downwards and descended into the cavernous sinus, whereas there was no cleft between the dura and the aneurysm.

Conclusions
Fusion images with 3D-MR cisternography and MRA yield clear visualization of the boundary between the CSF and cavernous sinus; this boundary can be used as the site of the DDR. This imaging technique might help to provide detailed information in paraclinoid aneurysms about their positional relationship to the roof of the cavernous sinus. The clinical bene-

fits of this method might be great when considering treatment options for unruptured ICA aneurysms on the basis of not only the size of aneurysm but also the potential risk for SAH.

References

1. Hitotsumatsu T, Natori Y, Matsushima T, et al. **Micro-anatomical study of the carotid cave**. *Acta Neurochir (Wien)* 1997;139:869–74
2. Oikawa S, Kyoshima K, Kobayashi S. **Surgical anatomy of the juxta-dural ring area**. *J Neurosurg* 1998;89:250–54
3. Beretta F, Sepahi AN, Zuccarello M, et al. **Radiographic imaging of the distal dural ring for determining the intradural or extradural location of aneurysms**. *Skull Base* 2005;15:253–61
4. Stuckey SL, Harris AJ, Mannolini SM. **Detection of acoustic schwannoma: use of constructive interference in the steady state three-dimensional MR.** *AJNR Am J Neuroradiol* 1996;17:1219–25
5. Casselman JW, Kuhweide R, Deimling M, et al. **Constructive interference in steady state-3DFT MR imaging of the inner ear and cerebellopontine angle.** *AJNR Am J Neuroradiol* 1993;14:47–57
6. Korogi Y, Takahashi M, Mabuchi N, et al. **Intracranial aneurysms: diagnostic accuracy of MR angiography with evaluation of maximum intensity projection and source images.** *Radiology* 1996;199:199–207
7. Nemec SF, Donat MA, Mehrain S, et al. **CT-MR image data fusion for computer assisted navigated neurosurgery of temporal bone tumors.** *Eur J Radiol* 2007;62:192–98
8. Satoh T, Omi M, Ohsako C, et al. **Differential diagnosis of the infundibular dilation and aneurysm of internal carotid artery: assessment with fusion imaging of 3D MR cisternography/angiography.** *AJNR Am J Neuroradiol* 2006;27:306–12
9. Kim JM, Romano A, Sanan A, et al. **Microsurgical anatomic features and nomenclature of the paraclinoid region**. *Neurosurgery* 2000;46:670–80; discussion 680–82
10. Kobayashi S, Kyoshima K, Gibo H, et al. **Carotid cave aneurysms of the internal carotid artery.** *J Neurosurg* 1989;70:216–21
11. Thines L, Delmaire C, Le Gars D, et al. **MRI location of the distal dural ring plane: anatomoradiological study and application to paraclinoid carotid artery aneurysms.** *Eur Radiol* 2006;16:479–88
12. Thines L, Gauvrit JY, Leclerc X, et al. **Usefulness of MR imaging for the assessment of nonophthalmic paraclinoid aneurysms.** *AJNR Am J Neuroradiol* 2007;29:125–29
13. Punt J. **Some observations on aneurysms of the proximal internal carotid artery.** *J Neurosurg* 1979;51:151–54
14. Gonzalez LF, Walker MT, Zabramski JM, et al. **Distinction between paraclinoid and cavernous sinus aneurysms with computed tomographic angiography.** *Neurosurgery* 2003;52:1131–37
15. Hashimoto K, Nozaki K, Hashimoto N. **Optic strut as a radiographic landmark in evaluating neck location of a paraclinoid aneurysm.** *Neurosurgery* 2006;59:880–95
16. Ito K, Hongo K, Kakizawa Y, et al. **Three-dimensional contrast medium-enhanced computed tomographic cisternography for preoperative evaluation of surgical anatomy of intradural paraclinoid aneurysms of the internal carotid artery: technical note.** *Neurosurgery* 2002;51:1089–92
17. Hirai T, Kai Y, Morioka M, et al. **Differentiation between paraclinoid and cavernous sinus aneurysms with contrast-enhanced 3D constructive interference in steady-state MR imaging.** *AJNR Am J Neuroradiol* 2008;29:130–33
18. Satoh T, Omi M, Ohsako C, et al. **Influence of perianeurysmal environment on the deformation and bleb formation of the unruptured cerebral aneurysm: assessment with fusion imaging of 3D MR cisternography and 3D MR angiography.** *AJNR Am J Neuroradiol* 2005;26:2010–18
19. Yasargil MG. **Intracranial arteries**. In: Yasargil MG, ed. *Microneurosurgery. Clinical Considerations, Surgery of the Intracranial Aneurysms and Results.* Vol. 2. Stuttgart: Thieme; 1984
20. al-Rodhan NR, Piepgras DG, Sundt TM Jr, et al. **Transitional cavernous aneurysms of the internal carotid artery.** *Neurosurgery* 1993;33:993–96; discussion 997–98